Polarization Multiplexing for Bidirectional Imaging

Oana G. Cula Kristin J. Dana* Dinesh K. Pai Dongsheng Wang
Computer Science Department
*Electrical and Computer Engineering Department
Rutgers University
Piscataway, NJ, USA

{oanacula,kdana}@caip.rutgers.edu,{dpai,dswang}@cs.rutgers.edu

Abstract

Our goal is to incorporate polarization in appearance-based modeling in an efficient and meaningful way. Polarization has been used in numerous prior studies for separating diffuse and specular reflectance components, but in this work we show that it also can be used to separate surface reflectance contributions from individual light sources. Our approach is called ***polarization multiplexing*** and it has significant impact in appearance modeling and bidirectional imaging where the image as a function of illumination direction is needed. Multiple unknown light sources can illuminate the scene simultaneously, and the individual contributions to the overall surface reflectance can be estimated. To develop the method of polarization multiplexing, we use a relationship between light source direction and intensity modulation. Inverting this transformation enables the individual intensity contributions to be estimated. In addition to polarization multiplexing, we show that phase histograms from the intensity modulations can be used to estimate scene properties including the number of light sources.

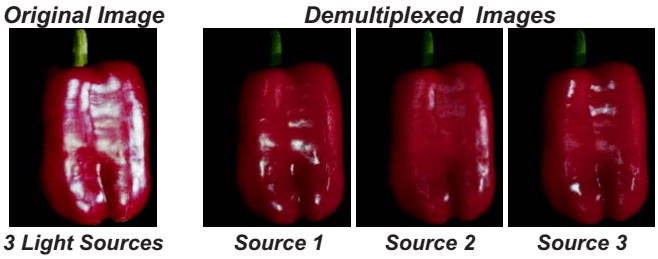

Figure 1. The pepper viewed with multiple light sources (left). Demultiplexed images that show the pepper as it would appear when illuminated by individual light sources separately (center and right).

1 Introduction

Polarization of reflected light provides a wealth of information not available in scalar intensity images. It is well known that polarization of light is a useful quantity for separating surface reflectance from body reflectance because surface reflectance maintains the polarization of the source, while body reflectance becomes depolarized. Appearance-based modeling requires images from multiple illumination and viewing directions, so bidirectional imaging is a common tool for capturing appearance [1, 20, 9, 8, 7, 14, 2]. In certain modeling tasks, it is important to separate the body and surface reflectance components to determine how each varies with illumination and view. For example, these two components may be interpolated differently for the appearance-based representation. The surface component contains roughness that changes appearance abruptly with illumination and view (high frequency variations), while the subsurface component is more diffuse (low frequency variations). Therefore the surface component requires a denser sampling of the illumination/view space. One area where layered representations has become particularly useful is in modeling the appearance of human skin [5, 13, 4, 6]. The particular use of polarization in image-based modeling has received sparse attention in the literature. Our goal is to create methods to accomplish polarized bidirectional imaging and to develop new algorithms in this domain.

Polarization of reflected light has been used in numerous ways by vision researchers. The polarization angle of reflected light has been used as a cue for image segmentation [22, 21], for shape estimation [15, 16, 17, 10] and for separating diffuse and specular reflectance components [12, 4, 19]. At first glance, polarized bidirectional imaging may seem straightforward. One simply adds a polarizer on the source and sensors. However, capturing polarized images is not our only goal; we also wish to use polarization to parse the contribution of individual light sources from the aggregate image. We develop a novel method called *po-*

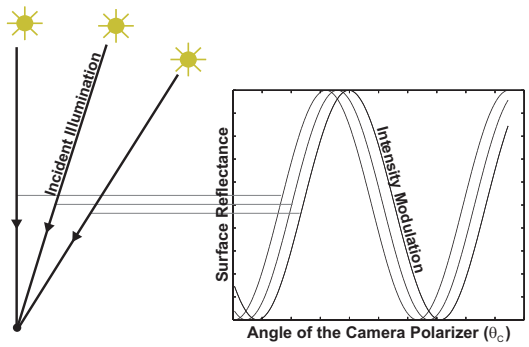

Figure 2. Because the light is polarized, there is a sinusoidal modulation on the intensity as a function of the camera polarizer angle. In addition, different angles of the incident illumination have modulation functions with different phases.

larization multiplexing to isolate the contribution of surface reflectance from the individual unknown light sources, as illustrated in Figure 1. It is well known that when linear polarizers are used on the light source and camera, the image intensity is modulated by a sinusoid. Further analysis reveals that when the plane of the polarizer is not restricted to be perpendicular to the illuminating ray, the modulating sinusoid also depends on the light source direction. We show that this modulation can be used to estimate the contribution from each light source even when all light sources are *unknown* and illuminate the scene *simultaneously*. Note that polarization multiplexing has a similar goal to illumination multiplexing [18], namely to determine the contribution from a single illumination direction. However, polarization multiplexing does not use an off/on spatial pattern of light sources but instead uses a rotating polarizer at the camera to get a pattern of modulation coefficients.

Because the phase of the intensity modulation depends on the light source direction, we can use phase clustering to reveal the number of light sources in the scene. Another method that estimates the light source distribution using polarization is described in [11], but the method is fundamentally different because it detects intensity maxima in the image to find specularities. For our approach, phase histograms are constructed and clusters reveal the light source number, as well as the extent of the light source.

2 Polarization Multiplexing

2.1 Overview

The surface reflectance from a point due to a set of light sources is modulated by a sinusoid that is a function of the camera polarizer angle and the light source direction, as illustrated in Figure 2. As an example, consider three light sources illuminating the scene. Let $[I(\theta_{c_1})\ I(\theta_{c_2})\ I(\theta_{c_3})\ ]$ be the measured images with three different rotation angles of the camera polarizer with all three light sources on. The contributions from the individual sources $[I(s_1)\ I(s_2)\ I(s_3)]$ are modulated with a sinusoid that depends on the camera polarizer angle and the light source direction. That is,

$$\begin{bmatrix} I(\theta_{c_1}) \\ I(\theta_{c_2}) \\ I(\theta_{c_3}) \end{bmatrix} = \begin{bmatrix} m_{11} & m_{12} & m_{13} \\ m_{21} & m_{22} & m_{23} \\ m_{31} & m_{32} & m_{33} \end{bmatrix} \begin{bmatrix} I(s_1) \\ I(s_2) \\ I(s_3) \end{bmatrix}. \quad (1)$$

The matrix M contains the modulation coefficients where each row corresponds to a fixed camera polarizer angle and each column corresponds to a fixed light source direction. Therefore demultiplexing can be done to obtain the individual contributions $[I(s_1)\ I(s_2)\ I(s_3)]$ by inverting the matrix M.

2.2 Intensity Modulation

We assume that for a given camera direction, the scene is viewed with multiple light sources. These light sources are behind a linearly polarized sheet as shown in Figure 4. Notice that this is a convenient setup because the light source can be controlled or uncontrolled. A second linear polarizer is placed on the camera. The polarizer at the light source is fixed and the polarizer at the camera can rotate. Assume there are N light sources given by s_j, $j \in [1..N]$. For a fixed camera position, we assume the viewing direction v is approximately constant over the image. Let l be the illumination direction; p_s is the light source polarizer direction; p_c is the camera polarizer direction; p is the polarization direction of the incident ray. We consider only the surface (specular) reflectance component that retains the polarization of the source. The body (diffuse) component of the reflectance becomes depolarized. The electric field vector of the light at the camera has a particular polarization direction in the imaging plane which we call q. Therefore the electric field vector at the camera polarizer is $E = |E|q$. With no camera polarizer the intensity captured by the camera sensor would be $I = EE^* = |E|^2$. When the light ray passes the camera polarizer the electric field vector becomes $E = (|E|\cos\theta)p_c$ where θ is the angle between the camera polarizer and the polarization of the light ray at the camera. The image intensity $I(\theta_c)$ with the camera polarizer rotated by θ_c is given by

$$I(\theta_c) = EE^* = |E|^2 \cos^2\theta_c. \quad (2)$$

This expression can be written to explicitly show the dependence on the camera polarizer angle θ_c and the light source s,

$$I(\theta_c, s) = (p_c \cdot q)^2 I(s), \quad (3)$$

where I(s) is the intensity in the image due to source s without the camera polarizer. To show the dependence on pixel coordinates (x, y),

$$I(x, y, \theta_c, s) = (p_c \cdot q)^2 I(x, y, s). \quad (4)$$

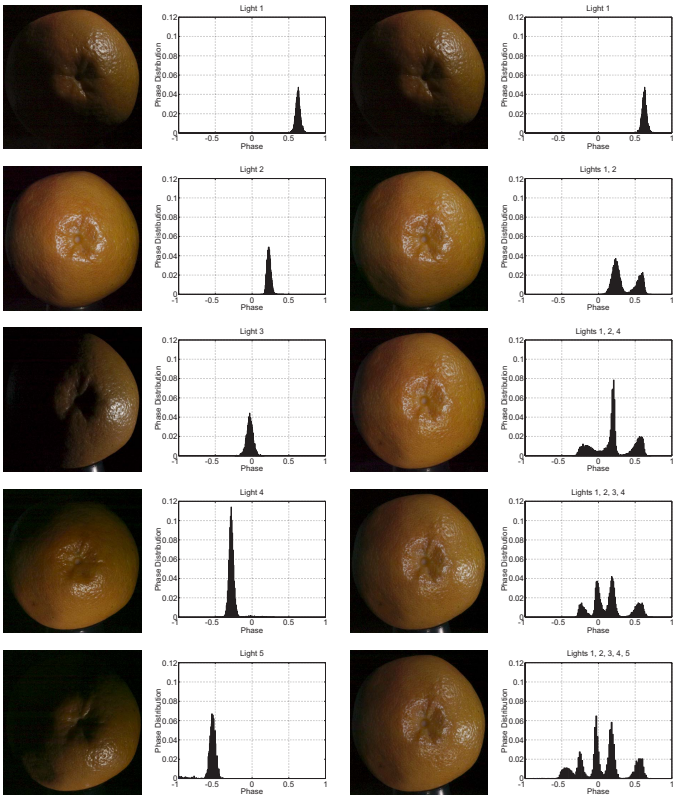

Figure 3. First column: the orange is illuminated by one light source, for five different light sources. Second column: the corresponding phase histograms for the five cases in the first column. Notice how distinct light directions give rise to a distinct cluster center the phase space (see Equation 7). Third column: the orange is imaged with five sources, added one at a time. Fourth column: the phase histograms corresponding to the five cases in the third column. Note that the number of clusters in the space of phase of the modulation curve equals the number of light sources illuminating the scene, therefore the phase carries information about the scene illumination.

We define a world coordinate frame W where the z-axis is aligned with p_s so that ${}^W p_s = [0, 0, 1]$. To get p, the polarizer direction p_s gets projected onto the plane perpendicular to the incident ray vector. That is, subtract from p_s the component parallel to l (assume l is the illumination direction) to get

$$p = p_s - (p_s \cdot l)\, l. \tag{5}$$

In world coordinates,

$${}^W p = \left(\begin{bmatrix} 0 \\ 0 \\ 1 \end{bmatrix} - l_z \begin{bmatrix} l_x \\ l_y \\ l_z \end{bmatrix} \right) = \begin{bmatrix} -l_x l_z \\ -l_z l_y \\ 1 - l_z^2 \end{bmatrix} \frac{1}{\sqrt{1 - l_z^2}}. \tag{6}$$

So we see that the polarization direction p depends on the illumination direction. Changing the illumination direction effectively rotates the polarization direction of the light vector at the camera (although all polarizers remain fixed). That is, different light directions have different modulation functions.

We arrange the camera so that the y-axis of the image plane is coincident with the z-axis of the world coordinate frame, and therefore coincident with p_s, the polarizer direction at the source. The angle that p makes with z_w in the plane perpendicular to l is the same as the angle q makes with z_w in the plane perpendicular to v (i.e. the image plane). This angle is given by

$$\phi = \arccos(p \cdot z_w) = \arccos(\sqrt{1 - l_z^2}). \tag{7}$$

The angle ϕ depends on l_z which in turn depends on the source s. For multiple sources the notation ϕ_j is used for $\phi(s_j)$. The intensity I due to source s_j is given by

$$I(\theta_c, s_j) = (p_c \cdot q)^2 I(s) = cos^2(\theta_c - \phi_j) I(s_j). \tag{8}$$

Notice that the intensity is a function of θ_c and l_z. Therefore the approach can separate sources that have different l_z values. Phases of the modulation functions do not vary for illumination vectors that lie in a line perpendicular to the axis of the polarizing screen. Pseudoinverse and singular value decomposition techniques are employed to avoid numerical problems in the implementation due to this degeneracy.

2.3 Demultiplexing Algorithm

We consider the situation where multiple light sources illuminate the scene simultaneously as shown in Figure 4. The aggregate intensity is given by

$$I(\theta_c) = \sum_{j=1}^{N} cos^2(\theta_c - \phi_j) I(s_j), \tag{9}$$

or

$$I(\theta_c) = \tfrac{1}{2} \textstyle\sum_{j=1}^{N} (1 + \cos 2\theta_c \cos 2\phi_j \tag{10}$$

$$+ \sin 2\theta_c \sin 2\phi_j) I(s_j), \tag{11}$$

where N is the number of sources.

Each camera polarization angle θ_c and each source direction gives a different attenuation curve. At a surface point, the incident light is the sum of individual light sources multiplied by a polarization attenuation coefficient that depends on the light source direction and the camera polarizer.

As an example, assume 4 sources and 4 camera polarizer angles $\theta_{c_1} \ldots \theta_{c_4}$. Then

$$I(\theta_c) = M\, I(s), \tag{12}$$

$$I(\theta_c) = M_a M_b I(s), \tag{13}$$

where

$$M_a = \begin{bmatrix} 1 & \cos 2\theta_{c_1} & \sin 2\theta_{c_1} \\ 1 & \cos 2\theta_{c_2} & \sin 2\theta_{c_2} \\ 1 & \cos 2\theta_{c_3} & \sin 2\theta_{c_3} \\ 1 & \cos 2\theta_{c_4} & \sin 2\theta_{c_4} \end{bmatrix} \tag{14}$$

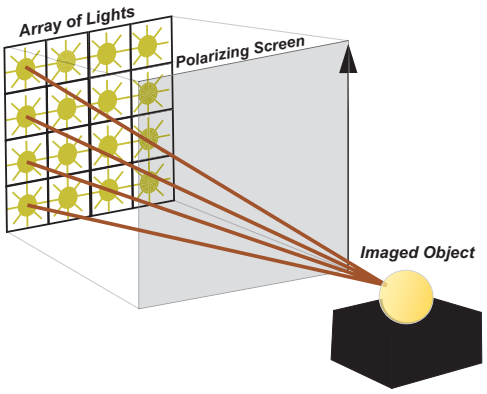

Figure 4. An object is imaged with multiple illumination directions and a polarized sheet is placed between the collection of light sources and the imaged object.

and

$$M_b = \begin{bmatrix} 1 & 1 & 1 & 1 \\ \cos 2\phi_1 & \cos 2\phi_2 & \cos 2\phi_3 & \cos 2\phi_4 \\ \sin 2\phi_1 & \sin 2\phi_2 & \sin 2\phi_3 & \sin 2\phi_4 \end{bmatrix}. \quad (15)$$

Note that since M can be factored into two matrices, we know that the rank of M cannot be greater than the rank of these factor matrices. That is

$$\begin{aligned} M &= M_a M_b, \\ rank(M) &\leq rank(M_a), \\ rank(M) &\leq rank(M_b) \end{aligned}$$

Therefore the rank of M is at most 3. So for each multiplexing stage, the individual contributions of three sources can be estimated. Demultiplexing is simply inverting Equation 12:

$$I(s) = M^{-1} I(\theta_c) \quad (16)$$

We extend the result to an arbitrary number of sources in Section 3.2.

3 Methods and Results

During the experiments, we imaged several objects, with various material properties or geometries. The imaging system we use for measurements is comprised of a Nikon D2H single lens reflex digital camera, equipped with Nikon Nikkor 28-80mm f/3.3-5.6G autofocus lens. The lens is augmented with a rotating linear polarizer glass filter. The light setup consists of 24 LED bulbs[1], arranged as a 6×4 array. Between the light array and the imaged scene we position a linearly polarizing screen[2], as shown in Figure 4.

[1] www.SuperBrightLeds.com

[2] Edmund Optics, Tech Spec Linear Polarizing Laminated Film

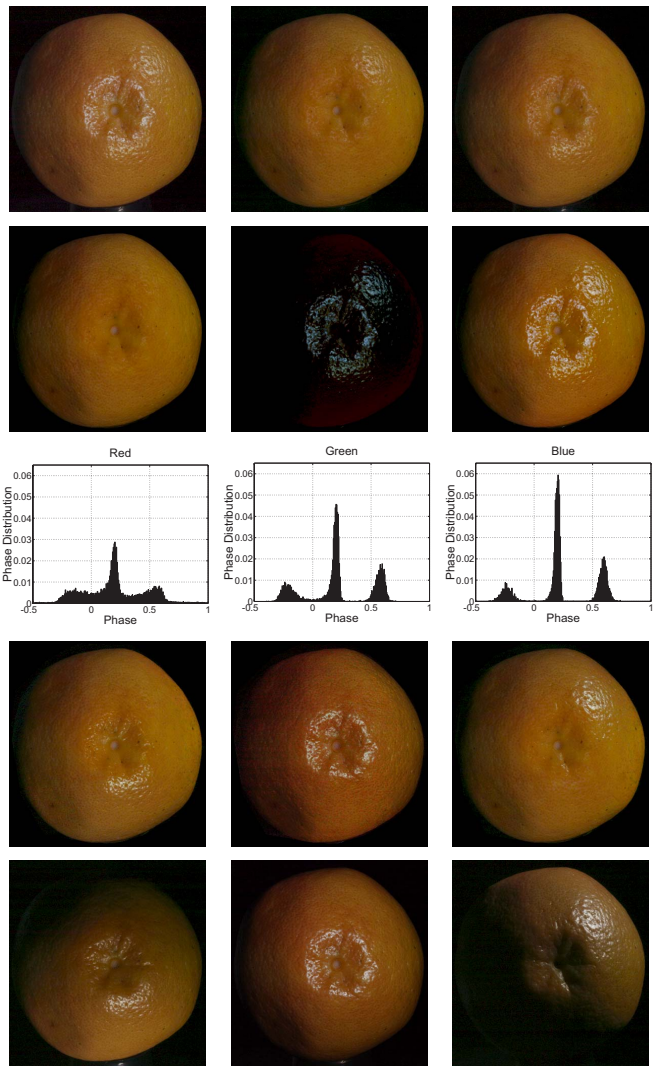

Figure 5. The orange is illuminated by three light sources, and the scene is imaged with three angles of the camera polarizer: $\{0, 2\pi/5, 4\pi/5\}$. First row: the input images used for decomposing the diffuse and specular components, and for polarization demultiplexing. Second row: the diffuse component, the specular component, and the superposition of the latter two, obtaining the image of the scene with all specularities present and not attenuated by the polarizer at the camera. Third row: phase distribution for the specular points in the scene, for each color channel. Fourth row: the demultiplexed specularities, illustrated superimposed over the diffuse component. Fifth row: the ground truth for the demultiplexed images. Notice that indeed the demultiplexed specularities are similar to those in the ground truth images, indicating a successful demultiplexing.

3.1 Multiplexing with Three Sources

To construct matrix M of Equation 12 the camera polarizer angle θ_c and the sinusoid phase ϕ_j must be known. The camera polarizer angle θ_c is calibrated with respect to the camera. The modulation sinusoid at each pixel is estimated to produce a phase histogram. We estimate the source phase ϕ_j as the center of the modes in the the phase distribution. The light source position need not be known.

Polarization demultiplexing necessitates a linear camera, and we use the methods in [3] to estimate the camera response, such that we could translate the image intensities into reflectance space, where superposition is valid.

An orange is illuminated by three different light sources, and the scene is imaged with three directions for the linear polarizer at the camera: $\{0, 2\pi/5, 4\pi/5\}$. The first row of Figure 5 shows the input images used for both decomposing the body and surface reflectance, and for polarization demultiplexing. The separated components, i.e. diffuse and specular, are illustrated in second row of Figure 5, along with the superposition of these two. Note that in this final image, obtained by adding the body and surface reflectance, all specularities are present, as if the polarizer at the camera is not present. The phase distributions for the specular points in the scene, for each color channel (third row of Figure 5), show three modes, i.e. three illumination sources are detected. Given the input images (first row of Figure 5), and applying our polarization demultiplexing technique, we obtain the demultiplexed specularities, as shown in the fourth row of Figure 5. The demultiplexed specularities are shown superimposed over the body reflectance. The fifth row of the same figure shows the ground truth for the demultiplexed images, that is, the orange is illuminated with each of the three individual light sources. By comparing the fourth and fifth rows, observe that indeed the demultiplexed specularities are similar to those in the ground truth images, indicating successful demultiplexing. The diffuse component differs for ground truth images and the demultiplexed images, as expected, because polarization multiplexing works for the surface reflectance. The diffuse component as a function of illumination direction can be readily modeled with existing methods. One such method is illumination multiplexing [18], which determines the contribution to the global reflectance from a single illumination direction. We can combine our method with illumination multiplexing, such that the contribution to the surface reflectance from a single light is resolved with polarization multiplexing, while the individual source contribution to the body reflectance is determined with illumination multiplexing.

A different scene, comprised of a red pepper, is similarly analyzed and illustrated in Figure 6. Again, comparison of the fourth and fifth rows of Figure 6 shows good results, i.e. the demultiplexed specularities match those in the ground truth images. The results are compelling, especially when one considers that the specularities are impossible to separate by visual inspection (see first row of Figure 6).

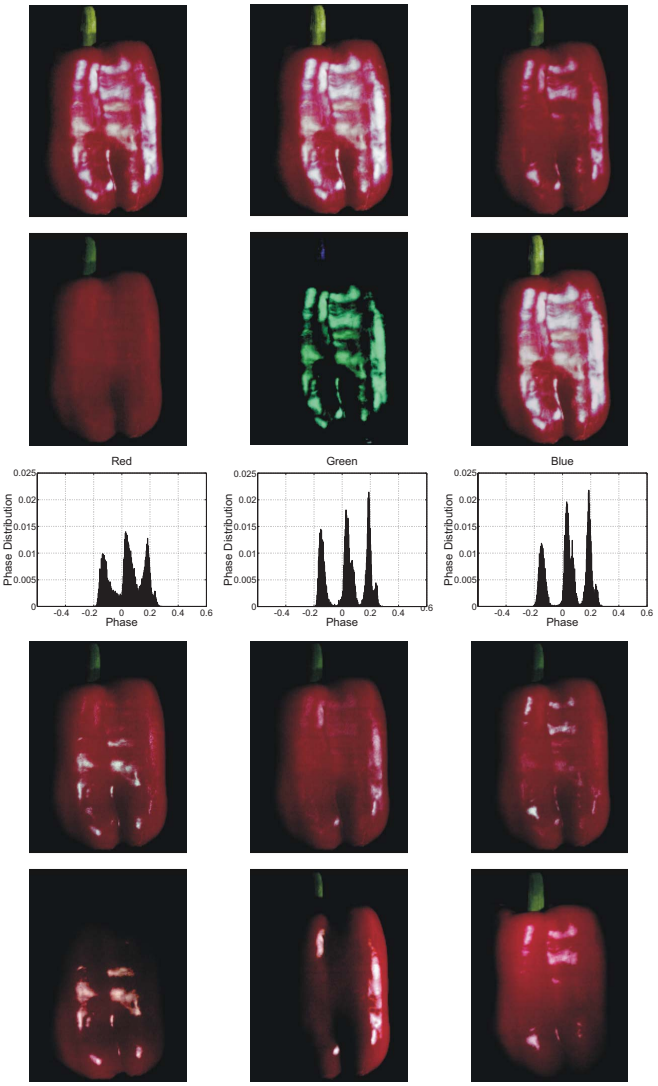

Figure 6. The pepper is illuminated by three different light sources, and the scene is imaged with three directions for the linear polarizer at the camera: $\theta_c = \{0, 2\pi/5, 4\pi/5\}$. First row: the input images employed for polarization demultiplexing. Second row: the diffuse component, the specular component, and the superposition of the latter two. Third row: phase distribution for the specular points in the scene, for each color channel. Fourth row: the demultiplexed specularities, shown with the diffuse component added. Fifth row: the ground truth for the demultiplexed images. Notice that the demultiplexed specularities are very similar to those in the ground truth images.

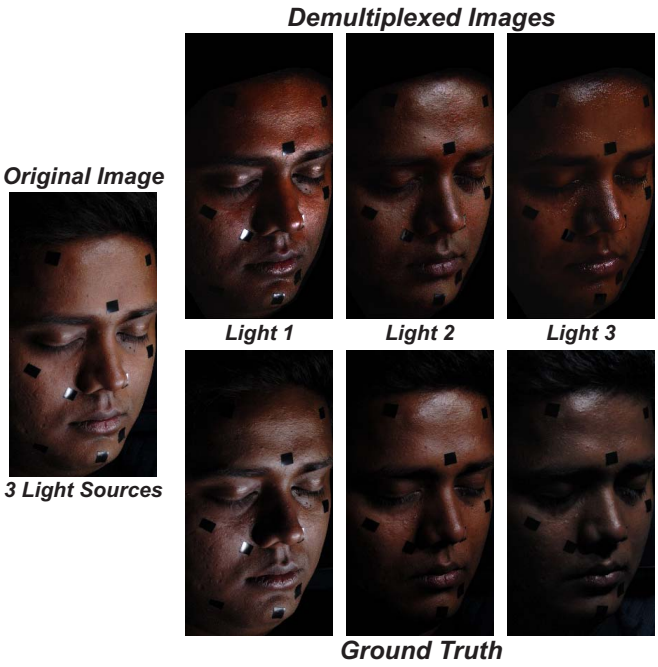

Figure 7. Demultiplexing results for a human face. The face is viewed with multiple light sources (left). Demultiplexed images that show the face as it would appear when illuminated by individual light sources separately (center and right, first row). Note that the surface reflection in the demultiplexed images matches the surface reflectance in the ground truth images (center and right, second row).

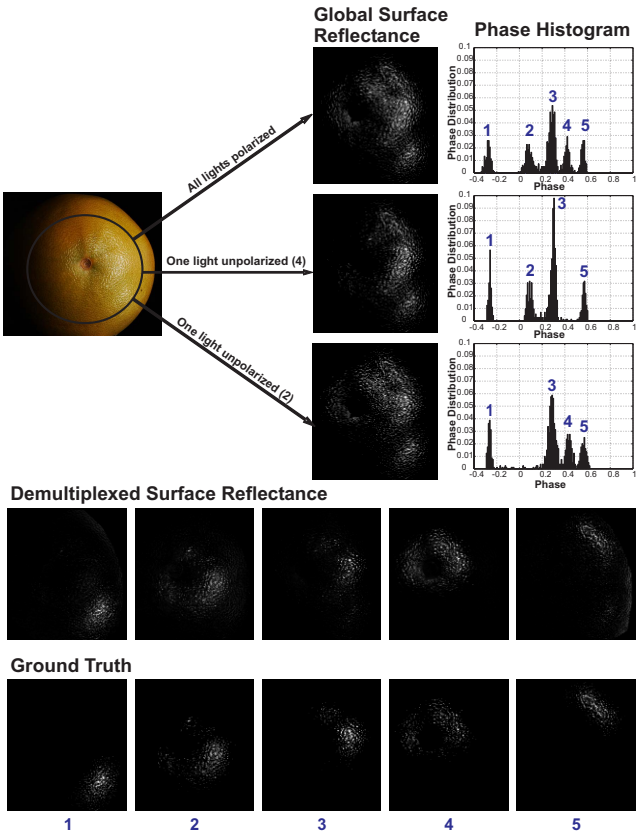

Figure 8. Multiplexing with more than three sources. The orange is illuminated by five sources. First, all five lights are polarized. The phase distribution presents five modes. Then, only four sources are polarized. The phase distribution presents four modes, showing that light 4 is not polarized. And finally, the scene is imaged with four polarized lights, while light 2 is not polarized. Demultiplexing is performed with these three sets of data. The results are very similar with the ground truth images.

Polarization demultiplexing is especially useful when imaging human faces. Acquiring good skin data is difficult, therefore a simplified measurement process is needed. Furthermore, when the scene is illuminated by multiple sources, the signal to noise ratio is better than when using a single source. The imaging process could be considerably shortened by imaging the skin surface with multiple light sources on, and then demultiplexing the surface reflectance due to each source. In Figure 7 we show results for a scene comprised of a human face illuminated simultaneously by three sources. The demultiplexed contributions to surface reflectance match the surface reflectance due to each source, illustrated by the ground truth images.

3.2 Multiplexing with More Than Three Sources

When the scene is illuminated by $N > 3$ light sources, matrix M in Equation 12 is still rank 3, therefore M is not invertible. We modify the polarization multiplexing method by adding $N - 3$ additional imaging sessions. During each additional imaging session one of the lights illuminating the scene is not polarized, and multiple images of the scene are acquired, as the polarizer at the camera is rotated. We use a linearly polarizing screen presenting a slit, such that by sliding the polarizing screen between the lighting environment and the scene, one light source remains unpolarized. The unpolarized light will give rise to surface reflectance which is not modulated by a sinusoid. We identify which light source is unpolarized by inspecting the phase distribution computed for each of the additional imaging sessions, i.e. by identifying the missing mode in the phase distribution. We construct M as follows: the first three rows are defined as in Equation 9; the following $N - 3$ rows are similarly defined, but they present a zero in the column corresponding to the unpolarized light source. Now matrix M has rank N, and it is invertible. By using Equation 16, we demultiplex the surface reflectance due to each of the N sources illuminating the scene.

Figure 8 exemplifies how polarization demultiplexing works for the case of five sources illuminating the scene. First, all sources are covered by the polarizing screen, and the corresponding phase histogram shows five modes, each corresponding to a source illuminating the scene. Then,

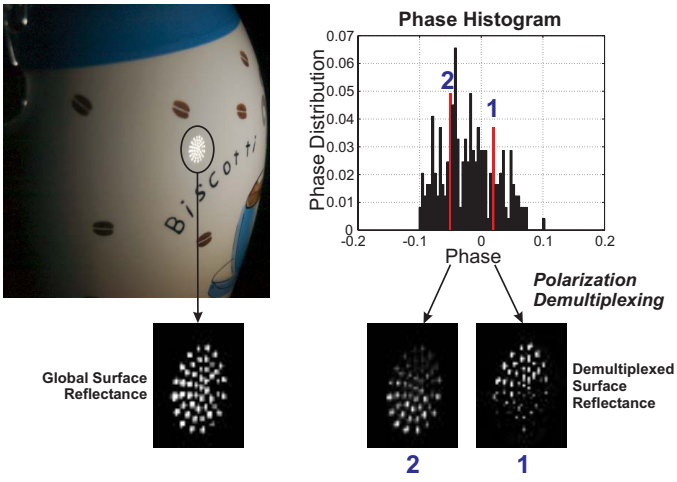

Figure 9. Multiplexing with one extended source. The jar is illuminated by one light source, and the phase distribution shows a single mode, as expected. By choosing two values for the phase, as shown by the two red bins, and performing polarization demultiplexing, the surface reflectance corresponding to two subdivisions of the light source is obtained. Notice that the demultiplexed specularities are indeed complementary.

the polarizing screen is placed between the scene and the lighting environment such that one source is not polarized. Again, the scene is imaged with three polarizer angles at the camera. The corresponding phase distribution presents four modes only, because the unpolarized source gives rise to unmodulated surface reflectance. From the phase distribution it can be seen that light 4 is not polarized. And finally, the scene is imaged again with the polarizer screen moved in a different position. The phase distribution presents four modes, showing that light 2 is not polarized. Demultiplexing is performed using these three sets of data. Figure 8 shows that the results are very similar with the ground truth images, acquired with just one source illuminating the scene.

3.3 Multiplexing with One Extended Source

In the real world the point light source assumption is often invalid, and we could think of a single light source as a cluster of multiple smaller sources. For example in our experiments we use LED bulbs, where each bulb is a cluster of 49 individual LEDs. In fact, the phase distribution appears as a Gaussian curve rather than an impulse function partly because the light source is not ideal.

In Figure 9 we image a ceramic jar with a single light source, and we illustrate the corresponding phase distribution for the modulation curves of the specular points in the scene. By sampling the phase distribution of the source in two values, as indicated by the red bins in Figure 9, and performing demultiplexing, we obtain refined specularities due to two subregions of the source. Figure 9 shows that indeed the demultiplexed specularities are complementary and due to different spatial contributions of the source.

3.4 Identifying the Number of Sources

We image a scene comprised of an orange, illuminated by only one light source, for five different sources, as shown in the first column of Figure 3. From the corresponding phase distributions, shown in the second column of Figure 3, we can see that different light directions give rise to a different locations of the clusters in phase space. Moreover, to test the separability of these modes in a more complex illumination configuration, the orange is imaged with five sources, added one at a time, as illustrated in the third column of Figure 3. That is, the first image in the column has one light source, the second has two light sources and so on. The corresponding phase distributions, plotted in the fourth column of the same figure, clearly show that the number of clusters in the phase space equals the number of sources illuminating the scene, therefore the phase carries information about the scene illumination.

4 Implications for Computer Vision and Graphics

In both computer vision and graphics, there is an increasing importance given to layered models, which decompose the image into body and surface reflectance, to determine how each varies with view and illumination. The body reflectance can be well modeled with known parametric models and a reduced number of images. On the other hand, surface reflectance is strongly dependent on the fine scale geometry of the scene, which is best measured with extensive bidirectional imaging. Thus there is a fundamental need for example-based models in modeling surface reflectance. Polarization multiplexing has a significant impact on bidirectional imaging and appearance-based modeling. Rather than imaging the scene with one light source at a time, the imaging process can be significantly simplified by illuminating the scene with multiple sources. Then polarization demultiplexing can be employed to isolate the contributions of individual sources to surface reflectance. Moreover, illuminating the scene with multiple sources allows a reduced exposure time at a good signal to noise ratio (especially important when imaging human subjects).

On the other hand, the scene might be simultaneously illuminated by a complex configuration of unknown light sources, which cannot be controlled. It is useful to know how each light source affects the appearance. Our polarization-based measurement protocol is especially fitted for this case, because in most cases we can place a polarizing screen between the scene and the lighting environment. The resulting measurements provide information about the number of sources illuminating the scene. Moreover, by using polarization multiplexing, one can separate

the effect of each source on surface reflectance.

As an example, consider a layered model for human face. The surface reflectance is strongly dependent on the fine scale geometry of skin, which is best captured with a large number of illumination directions. One important difficulty in building skin texture models is acquiring good data. Thus it is especially important for skin imaging to have a simplified measurement process. By illuminating the face with multiple light sources, and then demultiplexing the surface reflectance, the imaging process can be significantly shortened. Polarization demultiplexing does not isolate the contributions of different sources to the body reflectance, however the individual-specific diffuse component can be well modeled with just a few images and a parametric model. An accurate image-based model for skin surface reflectance is useful for both computer vision and graphics tasks. For example, in graphics accurate skin surface reflectance models improve realistic facial renderings, while in computer vision, face recognition can be greatly aided by the detailed skin surface reflectance, which complements the information given by the body reflectance.

Acknowledgement

This material is based upon work supported by the National Science Foundation under Grant No. 0092491, Grant No. 0085864, Grant IIS-0308157 and Grant EIA-0215887.

References

[1] O. G. Cula, K. J. Dana, F. Murphy, and B.K. Rao. Skin texture modeling. *International Journal of Computer Vision*, 62(1-2):97–119, April-May 2005.

[2] K. J. Dana, B. van Ginneken, S. K. Nayar, and J. J. Koenderink. Reflectance and texture of real world surfaces. *ACM Transactions on Graphics*, 18(1):1–34, January 1999.

[3] P. E. Debevec and J. Malik. Recovering high dynamic range radiance maps from photographs. *ACM SIGGRAPH*, pages 369–378, August 1997.

[4] P.E. Debevec, T. Hawkins, C. Tchou, H.-P. Duiker, W. Sarokin, and M. Sagar. Acquiring the reflectance field of a human face. *ACM SIGGRAPH*, pages 145–156, july 2000.

[5] A. Haro, B. Guenter, and I. Essa. Real-time, photo-realistic, physically based rendering of fine scale human skin structure. *Proceedings 12th Eurographics Workshop on Rendering*, pages 53–62, June 2001.

[6] H.W. Jensen. Digital face cloning. *SIGGRAPH 2003 Technical Sketch, San Diego*, July 2003.

[7] M. Koudelka, S. Magda, P. Belhumeur, and D. Kriegman. Image-based modeling and rendering of surfaces with arbitrary brdfs. *Proceedings of the IEEE Conference on Computer Vision and Pattern Recognition*, pages 568–575, 2001.

[8] M. L. Koudelka, S. Magda, P. N. Belhumeur, and D. J. Kriegman. Acquisition, compression and synthesis of bidirectional texture functions. *3rd International Workshop on Texture Analysis and Synthesis (Texture 2003)*, pages 59–64, October 2003.

[9] H. P. A. Lensch, J. Kautz, M. Goesele, Wolfgang Heidrich, and Hans-Peter Seidel. Image-based reconstruction of spatial appearance and geometric detail. *ACM Transactions on Graphics*, 22(2):234–257, April 2003.

[10] D. Miyazaki, M. Saito, Y. Sato, and K. Ikeuchi. Determining surface orientations of transparent objects based on polarization degrees in visible and infrared wavelengths. *Journal of the Optical Society of America*, 19(4):687–694, April 2002.

[11] D. Miyazaki, R. T. Tan, K. Hara, and K. Ikeuchi. Polarization-based inverse rendering in a single view. *International Conference on Computer Vision*, pages 982–987, 2003.

[12] S.K. Nayar, X.S. Fang, and T. Boult. Separation of reflection components using color and polarization. *International Journal of Computer Vision*, 21(3):163–186, February 1997.

[13] C. S. Ng and L. Li. A multi-layered reflection model of natural human skin. *Computer Graphics International*, pages 249–256, 2001.

[14] K. Nishino, Y. Sato, and K. Ikeuchi. Eigentexture method: Appearance compression and synthesis based on a 3d model. *IEEE Transactions on Pattern Analysis and Machine Intelligence*, 23(11):1257–1265, November 2001.

[15] S. Rahmann and N. Canterakis. Reconstruction of specular surfaces using polarization imaging. *Proceedings of the IEEE Conference on Computer Vision and Pattern Recognition*, pages 149–155, 2001.

[16] M. Saito, Y. Sato, K. Ikeuchi, and H. Kashiwagi. Measurement of surface orientations of transparent objects using polarization in highlight. *Proceedings of the IEEE Conference on Computer Vision and Pattern Recognition*, 1:381–386, 1999.

[17] Y. Y. Schechner, J. Shamir, and N. Kiryati. Polarization-based decorrelation of transparent layers: The inclination angle of an invisible surface. *International Conference on Computer Vision*, pages 814–819, 1999.

[18] Y.Y. Schechner, S.K. Nayar, and P. N. Belhumeur. A theory of multiplexed illumination. *International Conference on Computer Vision*, pages 808–815, 2003.

[19] N. Tsumura, N. Ojima, K. Sato, M. Shiraishi, H. Shimizu, H. Nabeshima, S. Akazaki, K. Hori, and Y. Miyake. Image-based skin color and texture analysis/synthesis by extracting hemoglobin and melanin information in the skin. *ACM Transactions on Graphics*, 22:770–779, July 2003.

[20] M. A. O. Vasilescu and Demetri Terzopoulos. Tensortextures. *ACM SIGGRAPH*, pages 336–342, 2004.

[21] L. B. Wolff and T. E. Boult. Constraining object features using a polarization reflectance model. *IEEE Transactions on Pattern Analysis and Machine Intelligence*, 13(7):635–657, 1991.

[22] L.B. Wolff. Polarization-based material classification from specular reflection. *IEEE Transactions on Pattern Analysis and Machine Intelligence*, 12(11):1059–1071, November 1990.